Kinetics of Silylene Insertion into N−H Bonds and the Mechanism and Kinetics of the Pyrolysis of Dimethylsilylamine

H. E. O'Neal,* M. A. Ring, J. G. Martin, and M. T. Navio

The Department of Chemistry, San Diego State University, San Diego, California 92182

Received: March 10, 1998; In Final Form: June 9, 1998

Product and kinetic data on the copyrolysis of silane with ammonia and of silane with dimethylamine are reported. The main products of the SiH_4/NH_3 reaction are disilane and silylamine, and the main products of the SiH_4/Me_2NH reaction are Si_2H_6 and Me_2NSiH_3. The silylamine products are produced by SiH_2 insertions into the N−H bonds of the amine reactants, and rate constants for this insertion lie in the $k_2 \sim 2 \times 10^9$ M^{-1} s^{-1} range, with no temperature dependence within the errors. Kinetic and product data on the pyrolysis of dimethysilylamine are also presented. Reactant loss followed reasonable first-order kinetics and produced rate constants consistent with Arrhenius parameters of log $A(sec^{-1}) = 12.64 \pm 0.98$ and $E = 48.02 \pm 3.1$ kcal/mol. A mechanism of reaction, based on the kinds of silylene intermediate reactions expected, is presented. Comparisons of mechanistic expectations with the product data, however, indicate a more complex reaction system.

Introduction

The deposition of thin films of silicon nitride (Si_3N_4) is very important to device fabrication in the microelectronics industry in which Si_3N_4 films are used as a capping material. Although most silicon nitride films are deposited via the reaction of SiH_4 with NH_3, it appears that the basic details of the gas-phase chemistry between SiH_4 and NH_3 are not known. In this paper, we present results from investigations the aim of which was to provide some understanding of the gas phase thermal processes occurring in the reaction of SiH_4 with NH_3 and higher alkylamines, e.g., Me_2NH. Silylamine is the initial product of the SiH_4/NH_3 reaction, therefore it was also of interest to study the decomposition of this substance. However, because silylamine has never been isolated, from which one can conclude that it is either thermally or reactively unstable under normal temperature (*T*) and pressure (*P*) conditions, we studied instead the decomposition of its closest stable analogue, silyldimethylamine (Me_2NSiH_3).

Experimental Section

The pyrolysis of SiH_4 with NH_3, of SiH_4 with Me_2NH, and of pure Me_2NSiH_3 were carried out in a heated 70.4 cm^3 cylindrical quartz reactor with direct capillary leak to a quadrupole mass spectrometer (MS). Product concentrations were determined from mass spectra obtained as a function of time. Up to five peaks were sampled sequentially in any scan and scan intervals were set at 7, 14, or 25 s depending on temperature. Details of the apparatus and of the operational procedures have been described.[1]

One of the problems peculiar to the Me_2NSiH_3 decomposition was a slow equilibration of the amine reactant pressures on expansion into the reaction cell. Thus, for example, although MS peaks for Argon (the internal analytical standard of these studies) reached maximum values within a few seconds, times for the reactant dimethylsilylamine peaks to maximize were on the order of 70 s. Selective absorption of the amine on the walls of the mass spectrometer seems the likely explanation. This nonequilibration effect was not a problem in the slower, lower temperature reactions, but did present some difficulties in the data analysis of the faster reactions.

Mass spectra from authentic samples of most of the species involved in these decompositions, namely of SiH_4, Si_2H_6, Si_3H_8, NH_3, Me_2NH, Me_2NSiH_3, and $(Me_2N)_2SiH_2$, were obtained so that mass spectra of the reaction products could be converted into product concentrations via sensitivity studies. Because authentic samples of silylamine were not available, its concentrations could not be so determined. Instead, silylamine was followed relative to disilane via MS peak ratios.

Me_2NSiH_3 was prepared by reaction of SiH_3Br and Me_2NH as described by Sujishi and Witz.[2] $(Me_2N)_2SiH_2$ was prepared by the same procedure from SiH_2Br_2 and Me_2NH. Both compounds were purified by trap-to-trap distillations under reduced pressure conditions and identified by their mass spectra (Table 1). The bromosilane reactants were prepared by reaction of SiH_4 and AgBr as described in an earlier paper.[3]

Results

The Reaction of SiH_4 with NH_3. Because the MS sensitivity of silylamine could not be determined, the reaction of SiH_4 with NH_3 was only studied under one set of conditions: with a $SiH_4/NH_3 = 1$ reactant mixture at 400 °C and a total pressure of 100 Torr. Initial products produced three multiplets, which in decreasing order of intensity (most intense in parentheses) were assigned as follows: Si_2H_6, $m/e = 56-62$ (58); SiH_3NH_2, $m/e = 42-47$ (44); $(SiH_3)_2NH$ or $SiH_3SiH_2NH_2$, 70−77 (74); and Si_3H_8 with peaks at the detection limit around $m/e = 90$. The silane and ammonia reactants were monitored at $m/e = 30$ and 31, and $m/e = 16$ and 17, respectively, silylamine was monitored at $m/e = 44$ and 47, and disilane was monitored at $m/e = 60$. A representative plot of the primary product data for this system, namely the ratio of silylamine to disilane (measured by their MS peak heights) as a function of time, is shown in Figure 1. The reason for the signal noise and instability of measurements made at long reaction times is unknown. Contributions of

10.1021/jp981436s CCC: $15.00
Published on Web 07/31/1998

TABLE 1: Mass Spectra of $(Me_2N)_2SiH_2$ and Me_2NSiH_3

	relative abundance		
m/e	$(Me_2N)_2SiH_2$	Me_2NSiH_3	ion
118	11.1		$(Me_2N)_2SiH_2^+$
117	3.4		$(Me_2N)_2SiH^+$
77		6.6	$Me_2NSi^{30}H_3^+$
76	4.4	9.9	$Me_2NSi^{29}H_3^+$
75	20.8	60.5	$Me_2NSiH_3^+$
74	73.6	100.0	$Me_2NSiH_2^+$
73	25.6	19.7	Me_2NSiH^+
72	20.0	42.8	Me_2NSiH^+
60	8.4	7.4	$MeNSiH_3^+$
58	25.2	23.7	$MeNSiH^+$
56	8.0	7.4	CH_2NSi^+
45	47.2	41.1	Me_2NH^+
44	100.0	60.5	Me_2N^+
42	47.2	68.4	$C_2H_4N^+$
31	8.0	20.9	SiH_3^+
30	8.0	9.9	SiH_2^+

unidentified, higher molecular weight products, particularly to the $m/e = 47$ peak, is a plausible explanation. Fortunately, data of the important regimes of reaction were far better behaved.

The Reaction of SiH_4 with Me_2NH. The reaction of SiH_4 with Me_2NH in an initial reactant ratio of $SiH_4/Me_2NH = 0.36$, was studied at three temperatures, 398, 422, and 453 °C, and at total pressures between 148 and 350 Torr. Product mass spectra again showed a series of multiplets which were assigned as follows: Si_2H_6, $m/e = 56-62$ (58); Me_2NSiH_3, $m/e = 73-75$ (74); Si_3H_8, $m/e = 84-92$ (89); $SiH_3SiH_2NMe_2$ or possibly $CH_2SiH_2CH_2N(-SiH_3)$, $m/e = 101-105$ (103); and $(Me_2N)_2SiH_2$, m/e around 118. Dimethylamine was monitored at $m/e = 45$, silyldimethylamine was monitored at $m/e = 75$, and bis-dimethylaminosilane was monitored at $m/e = 118$. Selective data for these studies are shown in Table 2; actual data collection was at more frequent intervals: 25 s intervals for the 398 °C runs and 7 s intervals for runs at the higher two temperatures.

The Me_2NSiH_3 Pyrolysis. The decomposition of Me_2NSiH_3 in a reactant mixture $Me_2NSiH_3/Ar = 5$ was studied at 393, 420, and 450 °C, and at total pressures between 40 and 100 Torr. Data of a typical run are shown in Table 3. In decreasing order of importance the major products were $(Me_2N)_2SiH_2$ ($m/e = 118$), H_2 ($m/e = 2$), and SiH_4 ($m/e = 30,31$). Reactant loss followed reasonable first-order kinetics over most of the reaction and least squares treatments of the data in the linear regions of the first-order plots yielded the following: $k = 9.02 \pm 1.51 \times 10^{-4}$ s^{-1} at 393 °C (4 runs); $k = 3.13 \pm 0.64 \times 10^{-3}$ s^{-1} at 422 °C (10 runs); $k = 1.39 \pm 0.63 \times 10^{-2}$ s^{-1} at 450 °C (4 runs). A least squares treatment of these rate constants gives: log A(sec^{-1}) = 12.64 ± 0.98 and $E = 48.02 \pm 3.1$ kcal/mol.

TABLE 2: Reactant Loss and Product Formation Data of the Dimethylamine/Silane Reaction[a,b]

		reactant and product concentrations in M × 10^3			
T (°C)	time (s)	SiH_4	Me_2NH	Si_2H_6	Me_2NSiH_3
398[c]	0	1.42	3.54		
	200	1.37	4.05	0.011	0.007
	400	1.33	4.05	0.021	0.027
	600	1.31	4.07	0.026	0.049
	800	1.29	4.08	0.029	0.077
	1200	1.26	4.06	0.032	0.117
421[d]	0	1.60	4.68		
	49	1.38	4.38	0.012	0.007
	98	1.36	4.40	0.022	0.024
	147	1.34	4.37	0.028	0.050
	196	1.32	4.33	0.032	0.078
	294	1.28	4.28	0.037	0.13
452[e]	0	1.40	4.39		
	14	1.22	3.80	0.014	0.017
	28	1.14	3.56	0.021	0.041
	56	1.06	3.40	0.031	0.106
	140	0.94	3.13	0.046	0.24
	210	0.87	2.96	0.052	0.27

[a] Reaction mixture composition was $Me_2NH/SiH_4/Ar = 3.84/1.39/1$. [b] Not all data are shown. Actual data intervals were 25 s at 398 °C and 7 s at the other two temperatures. [c] Runs at 398 °C were done at total pressures around 297 Torr. [d] Runs at 421 °C were done at total pressures around 320 Torr. [e] Runs at 452 °C were done at total pressures around 144 Torr.

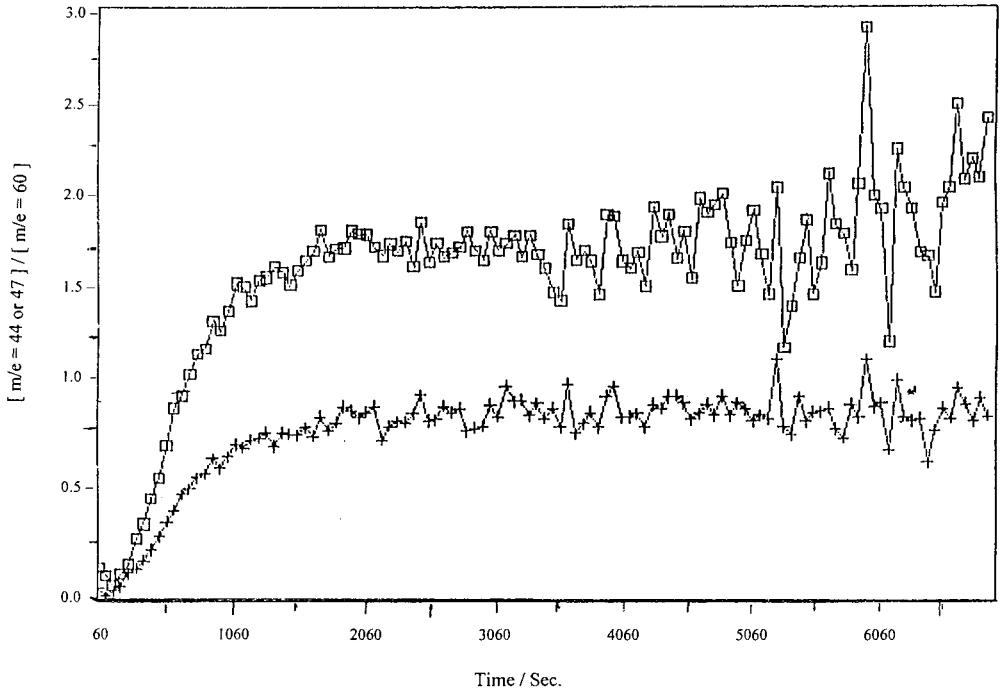

Figure 1. Silylamine/disilane product ratios in time for the SiH_4/NH_3 reaction. ⊡ SiH_3NH_2 ($m/e = 44$)/Si_2H_6 ($m/e = 60$); + SiH_3NH_2 ($m/e = 47$)/Si_2H_6 ($m/e = 60$).

TABLE 3: Representative Data of the Me_2NSiH_3 Pyrolysis (T = 421 °C)

	concentrations in M × 10^5				
t (s)	$[A]_{exp}$	$[A]_{calc}$[a]	$[H_2]$	$[SiH_4]$	$[(Me_2N)_2SiH_2]$
0		104	0	0	0
14	64.0[b]	98.5	2.0	0.7	4.0
28	77.4[b]	93.2	2.9	1.0	6.6
42	81.4[b]	88.2	3.4	1.2	8.3
56	80.9[b]	83.5	3.6	1.3	9.7
70	78.7	79.1	3.8	1.3	10.9
126	65.4	63.5	5.6	1.6	14.2
182	54.2	51.0	5.2	1.6	16.4
238	40.2	41.0	6.0	1.6	17.5
294	32.8	32.9	6.8	1.6	18.0
322	30.1	29.5	7.0	1.6	18.0
378	23.4	23.7	7.6	1.6	17.4
406	21.6	21.3	7.9	1.6	17.3
462	19.5[c]	17.1	8.3	1.5	16.2

[a] These reactant concentrations have been calculated from the least squares evaluated rate constant of the reaction, namely $k = 3.91 \times 10^{-3}$ s^{-1}. [b] These anamously low reactant concentration measurements are attributed to absorption of the reactant on the walls of the mass spectrometer. [c] The anomalously high reactant concentration measurement is attributed to high molecular weight contributions to the MS peak at $m/e = 118$ used to monitor the reactant.

Discussion

The SiH_4/NH_3 and SiH_4/Me_2NH Reactions. The reactions of silane with ammonia and of silane with dimethylamine occur in the same temperature range and at comparable rates as the pure silane decomposition.[4] It is therefore reasonable to expect that both reactions are initiated by the silane decomposition and that subsequent reactions are driven by silylene insertion/elimination reactions of the "usual" type. We therefore propose the mechanism of Scheme 1 to describe the gas-phase behaviors

Scheme 1: Possible Mechanism of a Silane/Amine Copyrolysis

$$SiH_4 + (M) \xrightarrow{1} SiH_2 + H_2 + (M)$$

$$SiH_2 + NHR_2 \underset{3}{\overset{2}{\rightleftarrows}} SiH_3NR_2 \xrightarrow{4} \text{products} \qquad R = H, Me$$

$$SiH_2 + SiH_4 \underset{6}{\overset{5}{\rightleftarrows}} Si_2H_6 \xrightarrow{7} SiH_3SiH + H_2$$

$$SiH_2 + Si_2H_6 \underset{9}{\overset{8}{\rightleftarrows}} Si_3H_8 \underset{11}{\overset{10}{\rightleftarrows}} SiH_3SiH + SiH_4$$

of these two systems.

Scheme 1 is consistent with the observed products and with the time frame of their formation. Thus, for example, the sigmoidal shape of the SiH_3NH_2/Si_2H_6 vs time plots of Figure 1 are completely consistent with Scheme 1. Initially, back reactions 3 and 6 are unimportant and production rates of silylamine and disilane are constant, hence a plot of their ratio, i.e., [m/e = 47 or 44]/[m/e = 60], is flat. This stage is very short-lived primarily because of an early onset of reaction 6. In the pure silane decomposition,[4] pseudo equilibrium conditions in reactions 5 and 6 (as well as 8−11) are established in the first 3−5% of silane conversion, with disilane reaching a maximum concentration which then slowly decays in accord with silane loss. In the present system, disilane also rapidly reaches a pseudo maximum condition but its concentration then gradually drifts up in time. This could be an artifact of higher molecular weight product contributions to the m/e = 60 mass peak. The period immediately following establishment of the disilane steady state is of most interest here because in this stage silylamine products continue to form without significant loss via their decomposition processes. Consequently, silylamine/disilane product ratios rise more or less linearly in time. That both reaction systems (SiH_4/NH_3 and SiH_4/Me_2NH) go through this stage is apparent in the plots of Figure 1 and data of Table 2. Only in the latter stages of reaction do the silylamine formation rates begin to plateau. In addition, the degree to which "plateauing" occurs seems to vary with temperature and with system. Thus, a falloff in silylamine production rates is very evident in the silane/ammonia system (see Figure 1 for the late stage leveling and completion of the sigmoidal behavior of the SiH_3NH_2/Si_2H_6 ratios in time), but is only apparent at the highest temperature and at the highest silane conversions in the silane/dimethylamine reaction system. By the mechanism, silylamine formation rates slow when silylamine decompositions (reactions 3 and 4) become important.

Rate expressions for silylamine and disilane formations are given by eqs 1 and 2, respectively.

$$d[SiH_3NR_2]/dt = k_2[SiH_2][NHR_2] - (k_3 + k_4)[SiH_3NR_2] \quad (1)$$

$$d[Si_2H_6]/dt = k_5[SiH_2][SiH_4] - (k_6 + k_7)[Si_2H_6] \quad (2)$$

If it were possible to establish the initial flat region of the silylamine/disilane product ratio, a direct measure of the desired k_5/k_2 rate constant ratio would result. However, this reaction stage is too short and product measurement errors too large to analyze reliably. However, the subsequent reaction stage, i.e., the stage after disilane reaches steady state but before silylamine products decompose significantly, can be meaningfully analyzed. For this stage, eqs 1 and 2 give equation 3.

$$dQ = [k_2(k_6 + k_7)/k_5]dt \quad (3)$$

where $Q = ([SiH_3NR_2]/[Si_2H_6]) \times ([SiH_4]/[NHR_2])$.

Thus, a plot of Q = vs t for data past the disilane maximum but prior to significant silylamine product decomposition should be linear with an intercept of zero and a slope of $k_2(k_6 + k_7)/k_5$. As predicted, Q vs t plots of the SiH_4/Me_2NH system data were indeed linear for reactions at the lower two temperatures, but as indicated above, these plots for runs at the highest temperature showed deviations from linearity at high silane conversions, see Figure 2.

Values of $k_2(k_6 + k_7)/k_5$ determined from slopes of the linear regions of the Q vs t plots of the silane/dimethylamine system are given in Table 4. Values for this same rate constant ratio relative to the silane/ammonia system are also shown. The latter, obtained from the slopes of the linear regions of the SiH_3NH_2 (m/e = 47 or 44)/Si_2H_6 (m/e = 60) product ratio vs time plots and the average reactant ratios, could be in error by a factor of 2 or more because of the uncertainties in the SiH_3NH_2 MS peak sensitivities.

Because Arrhenius parameters of k_6 and k_7, including the falloff behavior of reaction 6, are known[5,6] and rate constants for k_5 [7] under our reaction conditions can be estimated from the falloff of reaction 6, [5] values for k_2/k_5 and k_2 for both systems have been evaluated (Table 4 columns 5 and 7). Although the data at 398 °C suggest an inverse pressure dependence on the k_2/k_5 ratio, the pressure range and rather small falloff calculated for k_5 do not warrant the factor of 2 change determined in the ratio. It seems likely that the k_2/k_5 ratio spread is simply due to experimental error. Within the errors, $k_2/k_5 \sim 2 \times 10^{-2}$ and $k_2 \sim 2 \times 10^9$ M^{-1} s^{-1} for the silane/dimethylamine system,

TABLE 4: Evaluations of Relative and Absolute Rate Constants of SiH_2 Insertions into N—H Bonds

$SiH_4 + Me_2NH$ Reaction System

T (°C)	P (Torr)	slope[a]	$k_6/k_{6(\infty)}$[b]	k_2/k_5	$\langle k_2/k_5 \rangle$	k_2 (M^{-1} s^{-1})
398	297[f]	9.4×10^{-4}	0.95	1.7×10^{-2}		
	148	1.5×10^{-3}	0.89	2.9×10^{-2}		
	193	1.5×10^{-3}	0.90	2.8×10^{-2}	$2.2 \pm 0.6 \times 10^{-2}$[g]	$2.7 \pm 0.6 \times 10^{9}$
	310	8.4×10^{-4}	0.96	1.5×10^{-2}		
422	285[f]	3.6×10^{-3}	0.94	1.7×10^{-2}		
	361[f]	3.8×10^{-3}	0.95	1.7×10^{-2}		
	320	3.2×10^{-3}	0.95	1.5×10^{-2}	$1.6 \pm 0.1 \times 10^{-2}$[g]	$2.0 \pm 0.1 \times 10^{9}$
453	230	1.1×10^{-2}	0.88	1.1×10^{-2}		
	209	2.1×10^{-2}	0.85	2.1×10^{-2}		
	278	2.1×10^{-2}	0.90	2.0×10^{-2}	$1.7 \pm 0.4 \times 10^{-2}$[g]	$1.9 \pm 0.4 \times 10^{9}$
	262[f]	1.7×10^{-2}	0.89	1.7×10^{-2}		

$SiH_4 + NH_3$ reaction system

T (°C)	P (Torr)	slope[a]	$k_6/k_{6(\infty)}$[b]	k_2/k_5	$\langle k_2/k_5 \rangle$	k_2 (M^{-1} s^{-1})
400	100[d]	5.9×10^{-4}	0.78	1.1×10^{-2}		
	100[d]	7.4×10^{-4}	0.78	1.4×10^{-2}	$1.25 \pm 0.15 \times 10^{-2}$[g]	$1.3 \pm 0.4 \times 10^{9}$
	100[e]	1.7×10^{-3}	0.78	3.2×10^{-2}		
	100[e]	1.8×10^{-3}	0.78	3.4×10^{-2}	$3.30 \pm 0.1 \times 10^{-2}$[g]	$3.3 \pm 0.1 \times 10^{9}$

[a] Slopes of Q vs t plots $= k_2(k_6 + k_7)/k_5$ where $k_6 = k_{6(\infty)} \times k_6/k_{6(\infty)}$. [b] $k_{6(\infty)} = 10^{15.75} \times e^{-52200 \text{ cal/RT}}$ s^{-1} (ref 5); $k_{5(\infty)} = 1.3 \times 10^{11}$ M^{-1} s^{-1} (ref 7); $k_{6(10 \text{ Torr})} = 10^{15.13}$ x $e^{-50922 \text{ cal/RT}}$ s^{-1} (ref 5); $k_{6(150 \text{ Torr})} = 10^{15.38} \times e^{-51300 \text{ cal/RT}}$ s^{-1} (ref 5); $k_{6(500 \text{ Torr})} = 10^{15.67} \times e^{-51800 \text{ cal/RT}}$ s^{-1} (ref 5); $k_7 = 10^{15.81} \times e^{-56310 \text{ cal/RT}}$ s^{-1} (ref 6). ($k_6/k_{6(\infty)}$) and ($k_5/k_{5(\infty)}$) obtained by interpolation from the above parameters. [c] Slopes of (SiH_3NH_2/Si_2H_6) vs t plots $= k_2/k_5(k_6 + k_7)(NH_3/SiH_4)$. [d] Values shown are based on ($m/e = 47$)/($m/e = 60$) data. [e] Values shown are based on ($m/e = 44$)/($m/e = 60$) data. [f] These are the runs used in the Figure 2 plots. [g] Average values.

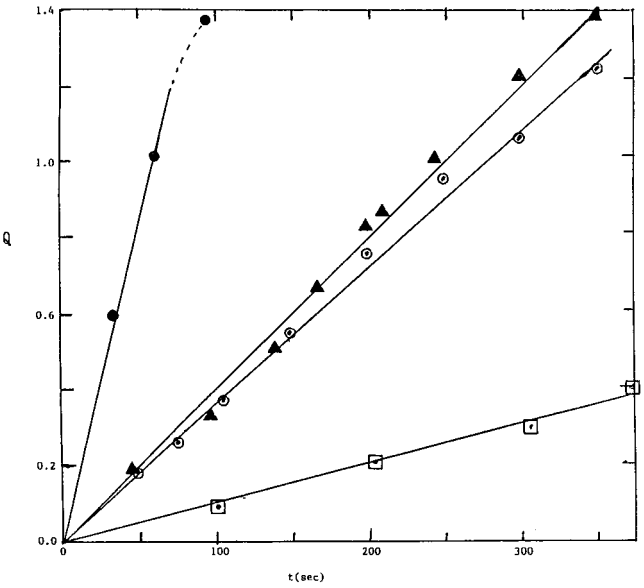

Figure 2. Q vs t plots of the SiH_4/Me_2NH reaction. $Q = (Me_2NSiH_3/Si_2H_6)/(SiH_4/Me_2NH)$. ⊡ Partial data for a representative run at 398 °C. ▲ and ⊙: Data from two representative runs at 422 °C. ●: Partial data from a representative run at 453 °C. The t and Q scales are respectively too short to show all the data points of the runs at 398 and 453. Nevertheless, beginning of curvatures in the 453 °C data plot is apparent. Data used for the plots are from the runs in Table 4.

with a possible negative activation energy for k_2. Similar values were obtained for the silane/ammonia system rate constants (Table 4), although these are subject to the uncertainties previously mentioned.

The k_2 values determined here are close to those found by Walsh et al.[8] for the reaction of Me_2Si with MeOH, namely $k = 7.1 \times 10^8$ M^{-1} s^{-1}. According to Walsh,[8] the latter reaction involves an oxygen nonbonding electron pair attack on the empty π orbital of silylene to form a dative bonded complex which then moves to a transition state involving H atom transfer from O to Si. Amine substrates, with their single nonbonding electron pair, should react with silylenes in a similar manner and possibly at comparable rates. Calculations by Melius and Ho[9] for the back reaction, i.e., the SiH_3NH_2 decomposition, also support this form of reaction.

From the SiH_3NH_2/Si_2H_6 product behavior of the silane/ammonia system (see Figure 1, for example), it is clear that the steady-state condition for silylamine is reached at 400 °C and high silane conversions. For this condition, eqs 1 and 2 lead to eq 4.

$$(k_3 + k_4) = [(k_2/k_5)(k_6 + k_7)(NH_3/SiH_4] \times [Si_2H_6/SiH_3NH_2] \quad (4)$$

Values of the terms in the first bracket on the right-hand side (RHS) follow from the slopes of the linear regions of silylamine/disilane vs t plots and the ratio of the reactant concentrations (see eq 3 or Table 4), and values of the second bracket on the RHS follow from the disilane/silylamine product ratios after they reach constant values, i.e., steady-state conditions for both products. Our SiH_4/NH_3 system data give average values for the terms of the first bracket of $6.7 \pm 0.7 \times 10^{-4}$ and $1.7 \pm 0.7 \times 10^{-3}$ ($m/e = 47$ or $m/e = 44$ for silylamine, respectively), and respective values for the terms of the second bracket are 1.1 ± 0.1 and 0.5 ± 0.05. Thus, silylamine decomposes with a composite rate constant ($k_3 + k_4$) of about $8.0 \pm 0.6 \times 10^{-4}$ s^{-1} at 400 °C. Because uncertainties in the silylamine MS sensitivities cancel in the product of the two RHS bracketed terms, this result is a fairly solid one. It appears, then, that silylamine decomposes at rates very similar to those of dimethylsilylamine. Thus, from the Arrhenius parameters for the latter's rate constant, $k(Me_2NSiH_3) = 11.1 \times 10^{-4}$ s^{-1} at 400 °C.

The Me_2NSiH_3 Pyrolysis. The Table 3 data illustrate several of the problems inherent to this system: slow equilibration of the reactant amine in the early stages of reaction, tailing-off of reactant loss in the final stages of reaction, and poor mass balances overall. The former is most pertinent to establishing the reaction kinetics and the latter is most pertinent to establishing the reaction mechanism. We have attributed the former behavior to reactant absorption on the mass spectrometer walls,

and it is reasonable to believe that the reactant loss tail-off effect is an artifact of higher molecular weight product contributions to the $m/e = 118$ peak.

Reactions at the two lower temperatures were relatively slow; the early stage nonequilibration of reactant was not a problem in determining the kinetics. Thus, one can see that the middle temperature run of Table 3 followed good first-order loss kinetics over 60% of the conversion range (between 20 and 80%), long enough to obtain a fairly accurate measure of the rate constant. Runs at the lowest temperature were even better behaved and yielded correspondingly better results. However, for runs at the highest temperature, reactant equilibration required almost a full half-life of reaction. Consequently, their rate constant errors are relatively large and this is reflected in correspondingly large errors of the reaction's Arrhenius parameters.

As for the mechanism of the Me_2NSiH_3 pyrolysis, a typical silane gas-phase reaction scheme like that shown in Scheme 2

Scheme 2: Possible Mechanism of the Silyldimethylamine Pyrolysis

$$H_3SiNMe_2 \xrightarrow{12} HSiNMe_2 + H_2$$

$$\xrightarrow{13} Me_2NH + SiH_2$$

$$HSiNMe_2 + H_3SiNMe_2 \xrightarrow{14} Me_2NSiH_2SiH_2NMe_2$$

$$Me_2NSiH_2SiH_2NMe_2 \xrightarrow{15} (Me_2N)_2SiH_2 + SiH_2$$

$$SiH_2 + H_3SiNMe_2 \xrightarrow{16} Si_2H_5NMe_2$$

$$Si_2H_5NMe_2 \xrightarrow{17} SiH_4 + HSiNMe_2$$

$$(M) + SiH_4 \xrightarrow{1} SiH_2 + H_2 + (M)$$

seems likely.

Paralleling the silane decomposition,[4] the initial steps of the silyldimethylamine pyrolysis (reactions 12 and/or 13) produce silylenes. These in turn should rapidly insert into the Si−H bond of the reactant to produce disilanes (reactions 14 and 16). Ab initio calculations of Melius and Ho[9] on the SiH_3NH_2 decomposition suggest that the enthalpy requirement for reaction 13 is considerably higher than that of reaction 12, hence barring any major surprises in their back reaction activation energies, it is likely that $k_{12} > k_{13}$. If this is the case, then the very low yields of H_2 observed would require the overall decomposition to be a long chain process. The unique feature of Scheme 2 is reaction 15, a 1,2-Me_2N shift disilane decomposition to produce the main reaction product: bis dimethylaminosilane or $(Me_2N)_2SiH_2$. This shift should be facilitated by the nonbonding electron pair on nitrogen. Similarly facilitated disilane decompositions are the Cl atom[10] and 1,2 OMe group shift processes.[11] The latter are among the fastest disilane decompositions known. Reaction 15 should therefore also be fast.

Reactions 14−17 constitute a chain, and this is one of the major problems with Scheme 2. It predicts a 50% yield of $(Me_2N)_2SiH_2$ and a combined H_2 and SiH_4 yield equal to that of $(Me_2N)_2SiH_2$. The data never meet the latter prediction and only meet the former (within the errors) in the very early stages of reaction. At longer times, $(Me_2N)_2SiH_2$ yields are well below 50%. It is interesting to note that the bis and silane product concentrations rise through maxima and then slowly decay, suggesting that both species have decomposition rates comparable to that of the reactant. This is clearly true for silane,[4] and we have found, through several test pyrolyses of the bis product, that it is also true for that substance. Because the expected decompositions of silane and the bis product both produce hydrogen, the low hydrogen yields are particularly difficult to understand. We can only offer the two surface reactions below as a possible explanation.

$$Me_2NSi_2H_5 \xrightarrow{18} Me_2NSi_2H_5\ (w) \rightarrow ?$$

$$Me_2NSiH_2SiH_2NMe_2 \xrightarrow{18} Me_2NSiH_2SiH_2NMe_2\ (w) \rightarrow ?$$

Here, aminodisilanes absorb and react on the surface without formation of gas-phase products. Similar processes appear to occur in the Si_3H_8 decomposition.[12]

Acknowledgment. The authors wish to thank the National Science Foundation for support of this research under grant no. CHE-9202437.

References and Notes

(1) Walker, K. L.; Jardine, R. E.; Ring, M. A.; O'Neal, H. E. *Int. J. Chem. Kinet.* **1998**, *30*, 69.
(2) Sujishi, S.; Witz, S. *J. Am. Chem. Soc.* **1954**, *76*, 4631.
(3) Hollandsworth, R. P.; Ingle, W. M.; Ring, M. A. *Inorg.Chem.* **1967**, *6*, 844.
(4) Purnell, H. J.; Walsh, R. *Proc. R. Soc. Ser. A* **1966**, *293*, 543. White, R. T.; Espino-Rios, R.L.; Rogers, D. S.; Ring, M. A.; O'Neal, H. E. *Int. J. Chem. Kinet.* **1985**, *17*, 1029.
(5) Martin, J. G.; Ring, M. A.; O'Neal, H. E. *Int. J. Chem. Kinet.* **1987**, *19*, 715.
(6) Dzarnoski, J.; Rickborn, S. F.; O'Neal, H. E.; Ring, M. A. *Organometallics* **1982**, *1*, 1217; Moffat, H. K.; Jensen, K. F.; Carr, R. W. *J. Phys. Chem.* **1992**, *96*, 7695.
(7) Becerra, R.; Frey, H. M.; Mason, B. P.; Walsh, R.; Gordon, M. S. *J. Am. Chem. Soc.* **1992**, *114*, 2751.
(8) Baggott, J. E.; Blitz, M. A.; Frey, H. M.; Lightfoot, P. D.; Walsh, R. *Int. J. Chem. Kinet.* **1992**, *24*, 127.
(9) Melius, C. F.; Ho, P. *J. Phys. Chem.* **1991**, *95*, 1410.
(10) Chernyshev, E. A.; Kamalenkov, N. G.; Bashkerova, S. A. *Zh. Obshch. Khim.* **1971**, *41*, 1175.
(11) Atwell, W. H.; Weyenberg, D. R. *J. Organomet. Chem.* **1966**, *5*, 594; *J. Am. Chem. Soc.* **1968**, *90*, 3438.
(12) Ring, M. A.; O'Neal, H. E. *J. Phys. Chem.* **1992**, *96*, 10848.